

# Lung Nodule Imaging using Micro CT

N. Niki, Y. Kawata, M. Fujii<sup>a</sup>, E. Matsui<sup>b</sup>, N. Moriyama<sup>c</sup>, Y. Tateno<sup>d</sup>

Univ. of Tokushima, <sup>a</sup>Toshiba IT & Control Systems

<sup>b</sup>Gifu Medical School, <sup>c</sup>National Cancer Center Hospital,

<sup>d</sup>National Institute of Radiological Science,

**Abstract--** We are developing a micro-computed tomography for imaging lung nodules. The purpose is to enhance the physician performance in accessing the micro architecture of the nodule for classification between malignant and benign nodules. The basic components of the micro CT consist of a microfocus X-ray source, a specimen manipulator, an image intensifier detector coupled to charge-coupled device camera and an image processing unit. Three-dimensional image reconstruction was performed on a slice by slice technique. A standard fan-beam convolution and back-projection algorithm was used to reconstruct the center plane intersecting the X-ray source. The preprocessing of the 3-D image reconstruction included the correction of the geometrical distortions and the shading artifact introduced by the image intensifier. The main advantage of the system is to obtain a high spatial resolution which ranges between  $5\text{ }\mu\text{m}$  and  $25\text{ }\mu\text{m}$ . In this work we report on preliminary studies performed with the micro CT for imaging resected tissues of normal and abnormal lung. Experimental results reveal micro architecture of lung tissues, such as alveolar wall, septal wall of pulmonary lobule, and bronchiole. From the results, the micro CT is expected to have interesting potentials for high confidential differential diagnosis.

## I. INTRODUCTION

Lung cancer is the leading cause of cancer deaths in the world. Early detection and treatment of lung cancers are crucially important to achieve high survival rate. There is hope in the possibility of early detection of lung cancer with the helical low-dose CT [1]. Computer-aided diagnosis is a promising approach to detect suspicious lesions on the thoracic CT images and alert physicians to these regions [2]. The detailed examinations of the small nodule lesions depend on the malignant potential. The differential diagnosis is ordinarily concluded by histological diagnosis from biopsy. It is often the case that biopsy technique becomes difficult according to nodule size is small. The advance of CT technology, such as a multi-slice CT scanner, provide fully 3-D images of pulmonary nodules with a high spatial resolution which ranges between  $300$  and  $500\text{ }\mu\text{m}$ . There has been a considerable amount of interest in the use of 3-D thoracic CT images to observe small pulmonary nodules for differential diagnosis [3]. A number of investigators have developed feature extraction and classification methods for characterizing pulmonary nodules [4]-[8]. However, these spatial resolutions have limitation for the quantitative diagnosis of micro tissues that form the small pulmonary nodule. Then, it becomes necessary to develop a micro-computed tomography which enables to analyze the micro architecture of lung tissues.

In recent years, there has been an increasing interest for developing the micro CT system. Rueggsegger et al. developed two systems based on multiple fan beam scanner [9]. One of their systems is realized for bone samples and small laboratory animals with a spatial resolution of  $20\text{ }\mu\text{m}$  and another system is used for the examination of patients with a spatial resolution of  $120\text{ }\mu\text{m}$ . Johnson et al. developed a volumetric micro CT with a spatial resolution of  $50\text{ }\mu\text{m}$  based on cone-beam scanner for quantification of pulmonary arterial wall [10]. Since the size of lung tissue such as alveolar wall is the order of several  $\mu\text{m}$ , a visualization of lung tissues requires the higher spatial resolution. Ritman et al reported that the spatial resolution of  $2\text{ }\mu\text{m}$  was achieved with synchrotron X-rays [11]. The spatial instruments require realizing the synchrotron-based system.

We present a micro CT system for analysis the micro architecture of lung tissues. The basic components consisted of a microfocus X-ray source, a specimen manipulator, an image intensifier detector coupled to charge-coupled device camera and an image processing unit. From results of the application to normal and abnormal lung tissues, we will demonstrate the availability of the micro CT for analysis of the lung micro architecture.

## II. METHODS

Fig. 1 shows the block diagram of the micro CT. The CT mainly consists of a microfocus X-ray source, a specimen manipulator, an image intensifier detector coupled to CCD camera and an image processing unit. The minimal size of the microfocus X-ray source is  $7\text{ }\mu\text{m}$ . The detector size of II can be chosen from three different sizes of 9, 6, 4.5 inch. The CCD array has three different areas corresponding to the II size with 1300 by 1030 pixels or 1300 by 512 pixels. The source-to-specimen distance and source-to-detector distance can be varied to obtain the desired magnification. The micromanipulator precisely positions the specimen table in the X-ray beams and rotates it under computer control through 360 degrees for projection data acquisition. This system can handle objects up to 200mm in diameter and up to 200mm in height. The acquisition time of 1800 views through 360 degrees is approximately one minute. The table position and motions and camera operations are under the control of the host computer with two CPUs (Pentium III Xeon, 500MHz) and 512MB main memory. The host computer receives the projection images and performs all data preprocessing, and image reconstruction is

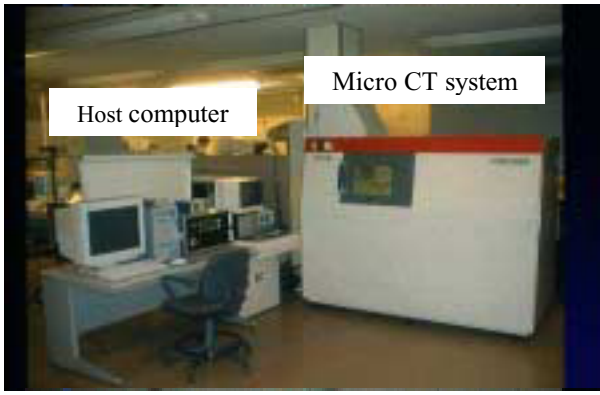


Fig.1. System overview

performed. Since the system geometry is a cone-beam geometry with a single circular orbit of the X-ray source, it is possible to apply cone beam reconstruction techniques [13] based on the Feldkamp algorithm [12]. These techniques provide approximate 3-D reconstructed images because they do not satisfy sufficiently the requirement for exactly 3-D image reconstruction [14]. In this CT, a standard fan-beam convolution and back-projection algorithm is used to precisely reconstruct the center plane intersecting the X-ray source. The preprocessing of the 3-D image reconstruction includes the correction of the geometrical distortions and the shading artifact introduced by II. The spatial resolution on the CT image ranges between  $5\ \mu\text{m}$  and  $25\ \mu\text{m}$ . The slice thickness is achieved up to the order of several  $\mu\text{m}$ .

### III. RESULTS

In the preliminary study, we investigate how the spatial resolution affects on quantitative diagnosis of micro lung tissues. We used three kinds of lung tissues, normal lung tissue, peripheral type of lung adenocarcinoma, and pulmonary adenocarcinoma in emphysematous lung. In order to compare between two different spatial resolutions in micro CT images, we reconstructed two volumetric micro CT images with different resolution of  $6\ \mu\text{m}$  and  $24\ \mu\text{m}$  for each lung tissue specimen. The measurement condition used in this experiment is as follows; the size of the microfocus X-ray :  $9\ \mu\text{m}$ , X-ray tube current :  $0.1\text{mA}$ , X-ray tube voltage :  $60\text{kV}$ , slice thicknesses :  $6\ \mu\text{m}$  and  $24\ \mu\text{m}$ , and the number of slice : 30slices. Each tissue is reconstructed into  $1024 \times 1024 \times 30$  cubic voxels (each voxel has  $6\ \mu\text{m}$  or  $24\ \mu\text{m}$  on a side).

Fig.2 shows the resected specimen, optical microscopic image, and soft X-ray image of the peripheral type of lung adenocarcinoma. In these figures the width of the alveolar wall where cancer cells are spread ranges from  $12\ \mu\text{m}$  to  $59\ \mu\text{m}$ . Fig. 3 shows the peripheral type of lung adenocarcinoma with two different spatial resolutions of  $24\ \mu\text{m}$  and  $6\ \mu\text{m}$ . Using the resolution of  $24\ \mu\text{m}$ , the alveolar wall of abnormal area is revealed due to wall thickening,

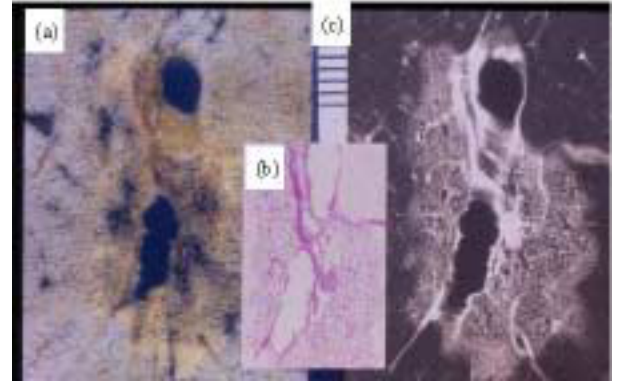
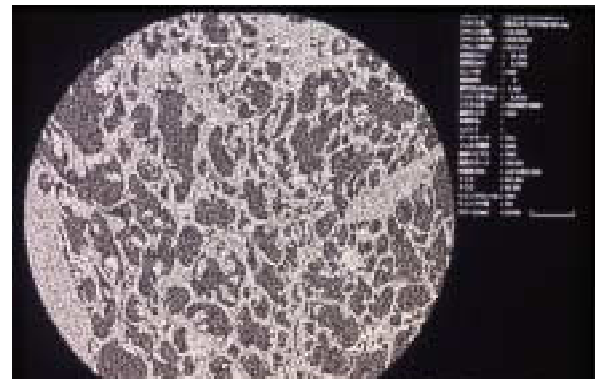


Fig.2. Abnormal tissue (peripheral type of lung adenocarcinoma) (a) Resected lung tissue. (b) Optical microscope image. (c) Soft X-ray image.



(a)



(b)

Fig.3. Micro CT images of the abnormal lung tissue. (peripheral type of lung adenocarcinoma) (a) Resolution :  $24\ \mu\text{m}$ . (b) Resolution :  $6\ \mu\text{m}$ .

while the alveolar wall of normal area can not be identified. With the resolution of  $6\ \mu\text{m}$ , the alveolar walls of both normal and abnormal areas can be easy to identify. Fig. 4 shows the 3-D display of the stacked slices of the peripheral type of lung adenocarcinoma with two spatial resolution of  $24\ \mu\text{m}$  and  $6\ \mu\text{m}$ . Using the resolution of  $24\ \mu\text{m}$ , the 3-D



(a)



(b)

Fig.4. 3-D display of the stacked Micro CT images of the abnormal lung tissue (peripheral type of lung adenocarcinoma) Resolution :  $24\ \mu\text{m}$  . (b) Resolution :  $6\ \mu\text{m}$  .

structure of the alveolar wall of abnormal area can be easy to identify. While with the resolution of  $6\ \mu\text{m}$  , the 3-D structure of the alveolar walls of both normal and abnormal areas are revealed.

Fig. 5 shows the resected specimen, optical microscopic image, and soft X-ray image of the pulmonary adenocarcinoma in emphysematous lung. In these figures the width of the alveolar wall where cancer cells are spread ranges from  $12\ \mu\text{m}$  to  $59\ \mu\text{m}$  . Fig. 6 shows slice images of the pulmonary adenocarcinoma in emphysematous lung with two different spatial resolution of  $24\ \mu\text{m}$  and  $6\ \mu\text{m}$  . Using the resolution of  $24\ \mu\text{m}$  , the alveolar wall of abnormal area is revealed due to wall thickening, while the alveolar wall of normal area can not be identified. With the resolution of  $6\ \mu\text{m}$  , the alveolar walls of both normal and abnormal areas can be easy to identify. Fig. 7 shows 3-D display of the stacked slices of the pulmonary adenocarcinoma in emphysematous lung with two spatial resolutions of  $24\ \mu\text{m}$  and  $6\ \mu\text{m}$  . Using the resolution of  $24\ \mu\text{m}$  , the 3-D structure of the alveolar wall of abnormal area can be easy to identify. While with the resolution of  $6\ \mu\text{m}$  , the 3-D structure of the alveolar walls of both normal and abnormal areas are revealed.

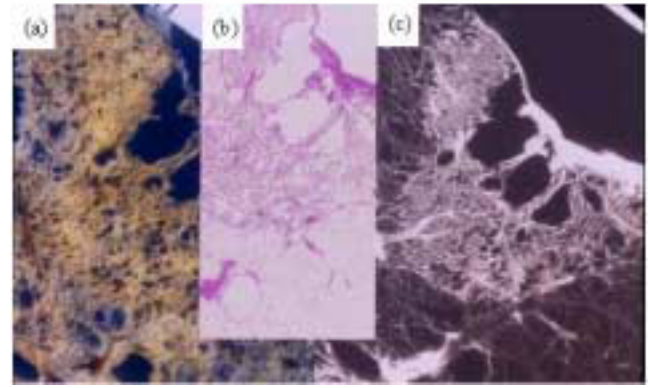
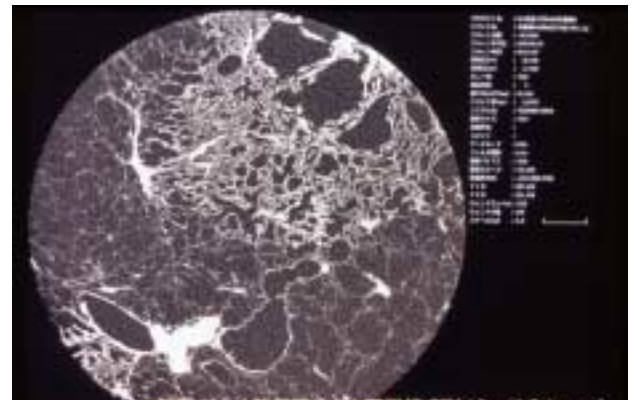


Fig. 5. Abnormal tissue (pulmonary adenocarcinoma in emphysematous lung) (a) Resected lung tissue. (b) Optical microscope image. (c) Soft X-ray image.



(a)

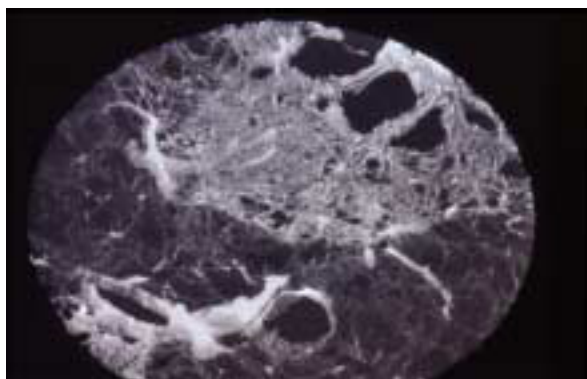


(b)

Fig.6. Micro CT images of the abnormal lung tissue (pulmonary adenocarcinoma in emphysematous lung) (a) Resolution :  $24\ \mu\text{m}$  . (b) Resolution :  $6\ \mu\text{m}$  .

#### IV. CONCLUSION

We have presented a micro CT for imaging pulmonary nodules. The spatial resolution of  $5\ \mu\text{m}$  allows physicians to



(a)



(b)

Fig.7. 3-D display of the stacked Micro CT images of the abnormal lung tissue (pulmonary adenocarcinoma in emphysematous lung) Resolution : 24  $\mu\text{m}$ . (b) Resolution : 6  $\mu\text{m}$ .

analyze the micro architecture of lung tissues, such as alveolar wall, septal wall of pulmonary lobule, and bronchiole. This CT allows for the first time to document changes of tissue components between normal and abnormal area. Future work we will have to show if structure indices are sufficient to predict the likelihood of malignancy of the pulmonary nodule. The high spatial resolution micro CT images provide the basic data set and then might help to improve the performance of physician diagnostic decisions.

#### REFERENCES

- [1] M.Kaneko, K.Eguchi, H.Ohmatsu, R.Kakinuma, T.Naruke, K.Suemasu, N. Moriyama, "Peripheral lung cancer: Screening and detection with low-dose spiral CT versus radiography," *Radiology*, 201, pp.798-802, 1996.
- [2] K.Kanazawa, Y.Kawata, N. Niki, H. Satoh, H. Ohmatsu, R. Kakinuma, M. Kaneko, N. Moriyama, K. Eguchi, "Computer-aided diagnosis for pulmonary nodules based on helical CT images," *Computerized Medical Imaging and Graphics*, 22, pp.157-167, 1998.
- [3] K.Mori, Y.Saitou, K.Tominaga, K.Yokoi, N.Miyazawa, A.Okuyama, M.Sasagawa, "Small nodular lesions in the lung periphery: New approach to diagnosis with CT," *Radiology*, 177, pp.843-849, 1990.
- [4] S.S.Siegelman, E.A.Zerhouni, F.P.Leo, N.F. Khouri, F.P. Stitik, "CT of the solitary pulmonary nodule," *AJR*, 135, pp.1-13, 1980.
- [5] D. Cavouras, P. Prassopoulos and N. Pantelidis, "Image analysis methods for solitary pulmonary nodule characterization by computed tomography," *European Journal of Radiology*, 14, pp.169-172, 1992.
- [6] M.F. McNitt-Gray, E.M.Hart, J. Goldin, C.-W. Yao, and D.R. Aberle, "A pattern classification approach to characterizing solitary pulmonary nodules imaged on high resolution computed tomography," *Proc. SPIE*, 2710, pp.1024-1034, 1996.
- [7] Y.Kawata, N.Niki, H.Ohmatsu, R.Kakinuma, K.Eguchi, M.Kaneko, N.Moriyama, "Shape analysis of pulmonary nodules based on thin-section CT images," *Proc. SPIE*, 3034, pp.967-974, 1997.
- [8] Y.Kawata, N.Niki, H.Ohmatsu, R.Kakinuma, K.Eguchi, M.Kaneko, N.Moriyama, "Quantitative surface characterization of pulmonary nodules based on thin-section CT images," *IEEE Trans. Nuclear Science*, 45, pp.2132-2138, 1998.
- [9] P. Ruegsegger, A. Kohlbrenner, D. Ulrich, A. Laib, "First results of a multiple fan-beam approach to analyze bone structure in vivo," *Proc. SPIE*, 3772, pp.55-62, 1999.
- [10] R. H. Johnson, R.C. Molthen, K.L. Karau, C.C. Hanger, S.T. Haworth, C.A. Dawson, and J.H. Linehan, "Analysis of 3D pulmonary microrangiograms," *Computer-Aided Diagnosis in Medical Images*, K. Doi, H. MacMahon, M.L. Giger and K.R. Hoffmann, eds., Elsevier Science, pp.349-376, 1999.
- [11] E.L. Ritman, S.M. Jorgensen, P.E. Lund, P.J. Thomas, J.H. Dunsmuir, J.C. Romero, R.T. Turner, and M.E. Bolander, "Synchrotron-based micro-CT of in situ biological basic functional units and their integration," *Proc. SPIE*, 3149, pp.13-24, 1997.
- [12] L.A. Feldkamp, L.C. Davis and J.W. Kress, "Practical cone-beam algorithm," *Journal of the Optical Society of America*, 1, pp.612-619, 1984.
- [13] Y. Kawata, N. Niki, H. Satoh, and T. Kumazaki, "Three-dimensional blood vessels reconstruction using a high-speed X-ray rotational projection system," *Trans. IEICE*, J76-D-II, pp.2133-2142, 1993.
- [14] B.D. Smith, "Image reconstruction from cone-beam projections: Necessary and sufficient conditions and reconstruction methods," *IEEE Trans. Medical Imaging*, MI-4, pp.14-25, 1985.